A magnetic-based dispersive micro-solid-phase extraction method using the metal-organic framework HKUST-1 and ultra-high-performance liquid chromatography with fluorescence detection for determining polycyclic aromatic hydrocarbons in waters and fruit tea infusions

Priscilla Rocío-Bautista[1], Verónica Pino[1,*], Juan H. Ayala[1], Jorge Pasán[2], Catalina Ruiz-Pérez[2], Ana M. Afonso[1]

[1]Departament of Chemistry - Analytical Division, University of La Laguna, Tenerife, 38206 Spain
[2]X Ray and Molecular Materials Lab (MATMOL), Physics Department, University of La Laguna, Tenerife, 38206 Spain

Abstract

A hybrid material composed by the metal-organic framework (MOF) HKUST-1 and Fe_3O_4 magnetic nanoparticles (MNPs) has been synthetized in a quite simple manner, characterized, and used in a magnetic-assisted dispersive micro-solid-phase extraction (M-d-µSPE) method in combination with ultra-high-performance liquid chromatography (UHPLC) and fluorescence detection (FD). The application was devoted to the determination of 8 heavy polycyclic aromatic hydrocarbons (PAHs) in different aqueous samples, specifically tap water, wastewaters, and fruit tea infusion samples. The overall M-d-µSPE-UHPLC-FD method was optimized and validated. The method is characterized by: its simplicity in both the preparation of the hybrid material (simple mixing) and the magnetic-assisted approach (~10 min extraction time), the use of low sorbent amounts (20 mg of HKUST-1 and 5 mg of Fe_3O_4 MNPs), and the low organic solvent consumption in the overall M-d-µSPE-UHPLC-FD method (1.5 mL of acetonitrile in the M-d-µSPE method and 2.8 mL of acetonitrile in the UHPLC-FD run). The resulting method has high sensitivity, with LODs down to 0.8 $ng \cdot L^{-1}$; adequate intermediate precision, with relative standard deviation values (RSD) always lower than 6.3% (being the range 5.9 – 9.0% in tap water for a spiked level of 45 $ng \cdot L^{-1}$, 6.1 – 14% in wastewaters for a spiked level of 45 $ng \cdot L^{-1}$, and 7.2 – 17% in fruit tea infusion samples for a spiked level of 45 $ng \cdot L^{-1}$); and adequate relative recoveries, with average

values of 82% in tap water, and 94% and 75% in wastewater and fruit tea infusion samples, respectively, if using the proper matrix-matched calibration.

Keywords: metal-organic frameworks; magnetic nanoparticles; dispersive micro solid-phase extraction; polycyclic aromatic hydrocarbons; environmental waters; fruit-tea infusions

*Corresponding author: Tel. +34 922318990. Email: veropino@ull.edu.es

P. Rocío-Bautista	procio@ull.es
J.H. Ayala	jayala@ull.es
J. Pasán	jpasang@ull.es
C. Ruiz-Pérez	caruiz@ull.es
A.M. Afonso	aafonso@ull.es

1. Introduction

The utilization of nanoparticles (NPs, 1–100 nm) is quite advantageous for chemical analysis given the intrinsic characteristics of these materials: high superficial area, unique reactivity, high chemical stability, and easiness of functionalization, among others [1,2]. Magnetic nanoparticles (MNPs) are a kind of NPs presenting superparamagnetism. The magnetic solid phase of MNPs mainly consists of iron minerals and magnetic iron oxides such as magnetite (Fe_3O_4) [3]. The use of MNPs has really increased the applicability of magnetic-facilitated extraction procedures since 1996 [4]. Analytical extraction approaches based on MNPs (using bare or coated MNPs to extract analytes) are advantageous over more classical solid-phase extraction approaches (SPE). Thus, MNPs-based extraction methods avoid filtration and centrifugation steps, because the extractant sorbent can be easily separated from the remaining components of the sample with the application of an external magnetic field [4-6]. The utilization of dispersive micro-SPE (d-μSPE) with the help of any agitation system (vortex, ultrasounds, stirring…), rather than static μSPE (sorbent amounts < ~500 mg), facilitates the transfer of the analytes to the sorbent material while reducing extraction times [7].

Bare MNPs are scarcely used in analytical extraction methods due to their high chemical reactivity, tendency to aggregation, easily oxidation in air, and quick biodegradation. Thus, coated and/or functionalized MNPs are commonly used [4-6] because they present higher chemical and colloidal stability. Besides, they have wider extraction capabilities, because other sorbent materials are incorporated generating a hybrid material. More common hybrid materials for magnetic-based d-μSPE include

70 silica (Fe_3O_4@SiO_2) [8,9], surfactants [10,11], molecular imprinted polymers
71 (Fe_3O_4@MIPs) [12,13], and carbon nanotubes (Fe_3O_4@CNTs) [14,15].

72 Metal-organic frameworks (MOFs) are a group of materials that are starting to
73 receive increasing attention in analytical chemistry [16,17] given their outstanding
74 properties: permanent nanoscale porosity, good thermostability, high surface area,
75 impressive tuneability (almost infinite combination of metals and organic linkers), and
76 uniform structure cavities [18]. Thus, several MOFs have been proposed as sorbent
77 materials in SPE [19,20], d-µSPE [7,21], solid-phase microextraction (SPME) [22-
78 24],…

79 MOFs have also been proposed in combination with MNPs in magnetic-based d-
80 µSPE (M-d-µSPE) approaches, mainly for the determination of metals [25-29].
81 Regarding the determination of organic compounds, it has been mainly described the
82 use of Fe_3O_4@SiO_2@MOF [30-32]. The use of MNPs without silica has only been
83 reported for polychlorinated biphenyls (PCBs) with the MOF MIL-100 [33] and using a
84 prior functionalization of Fe_3O_4 with mercaptoacetic acid (30 min each cycle, 30 cycles
85 overall), and for organophosphorus pesticides with the MOF MIL-101 [34] and using
86 the solvothermal method without any functionalization (~20 h).

87 The present work reports the utilization of the MOF HKUST-1 in combination
88 with MNPs, in a M-d-µSPE method with ultra-high performance liquid chromatography
89 (UHPLC) and fluorescence detection (FD) for the determination of eight heavy
90 polycyclic aromatic hydrocarbons (PAHs). The analytical applications is carried out
91 with environmental waters (tap water and wastewaters), and with fruit tea infusion in
92 which PAHs have been reported [35,36]. It is important to highlight that the preparation
93 of the hybrid material HKUST@Fe_3O_4 is accomplished without ensuring any kind of
94 chemical binding through a reaction: both materials are simply mixed with the aqueous

sample. Thus, the overall method is quite simple, not only for the use of a magnetic-based approach but also for the easiness of preparation of the hybrid sorbent material.

2. Experimental

2.1. Chemicals, reagents, materials and samples

The eight PAHs studied in this work were: benzo[a]anthracene (BaA), chrysene (Chy), benzo[b]fluoranthene (BbF), benzo[k]fluoranthene (BkF), benzo[a]pyrene (BaPy), dibenz[a,h]anthracene (DahA), benzo[ghi]perylene (BghiPer), and indeno[1,2,3-cd]pyrene (I(1,2,3-cd)Py). BaA, BbF, BaPy, DahA and I(1,2,3-cd)Py were supplied by Dr. Ehrenstorfer GmbH (Augsburg, Germany) as individual standard solutions in acetonitrile with a concentration of 10 $mg \cdot L^{-1}$. Chy (98%) and BghiPer (98%) were supplied as solids by Aldrich (Milwaukee, Wisconsin, USA). BkF (99%) was supplied as solid by Fluka Chemika (Buchs, Switzerland). These solids were used to prepare standard solutions with concentrations of 80 $mg \cdot L^{-1}$ for BkF, 92 $mg \cdot L^{-1}$ for Chy, and 80 $mg \cdot L^{-1}$ for BghiPer, all kept at 4 ºC and also protected from light. These eight standard solutions were used to prepare a mixture standard solution in acetonitrile with all 8 PAHs with a concentration of 1 $mg \cdot L^{-1}$. Such standard mixture solution was used to spike water (ultrapure water, tap water or wastewaters) and fruit-tea infusion samples, as well as to prepare working aqueous standard solutions of all PAHs at $\mu g \cdot L^{-1}$ levels.

Ultrapure Milli-Q water was obtained by a water purification system A10 MilliPore (Watford, UK). Acetonitrile (ACN) was obtained from VWR (Llinars del Vallés, Spain) with LC-MS purity grade. Hexane was acquired to Sigma-Aldrich

120 (Steinheim, Germany) with Chromasolv® grade. Trichloromethane (TCM) and
121 dichloromethane (DCM) were supplied by Panreac (Barcelona, Spain) with pro-analysis
122 purity grade.

123 HPLC mobile phases were filtered before use using Durapore® membrane filters
124 of 0.20 μm, supplied by Sigma Aldrich.

125 Absolute ethanol PRS 99.5%, supplied by Panreac, copper (II) nitrate
126 hemipentahydrate and benzene-1,3,5-tricarboxylic acid (trimesic acid) (95%), supplied
127 by Sigma-Aldrich, were utilized in the synthesis of HKUST-1.

128 Iron (III) chloride hexahydrate ($FeCl_3 \cdot 6H_2O$) (≥99%), iron (II) chloride
129 tetrahydrate ($FeCl_2 \cdot 4H_2O$) (≥99%), sodium hydroxide (≥98%), and hydrochloric acid
130 (≥37%), all from Sigma-Aldrich, were required in the synthesis of Fe_3O_4 magnetic
131 nanoparticles.

132 0.2 μm syringe Milex® Durapore® PVDF (Polyvinylidene fluoride) were
133 purchased from Sartorius Stedim Biotech (Goettingen, Germany), and used before any
134 UHPLC injection of samples and standards.

135 A prism (5 cm × 2 cm × 2 cm) NdFeB magnet was purchased to ENES Magnesy
136 Pawel Zientek (Warszawa, Poland).

137 Tap water was taken at the laboratory and three wastewaters were supplied by an
138 environmental monitoring laboratory belonging to the University. Wastewaters were
139 directly sampled at the wastewater treatment plant. In all the cases, sampling was
140 carried out while avoiding the formation of bubbles, and using clean amber glass bottles
141 of 100 mL in volume. Samples were also maintained in a portable fridge until they
142 reached the laboratory, and then maintained in the dark at 4 ºC for no more than 48 h,
143 before being analyzed.

Three fruit-tea samples were bought in a local supermarket, being its fruity content specifically composed of: apple, elder flower, mallow flower, plum and lemon (fruit-tea 1); Guarana, ginger and raspberry (fruit-tea 2); and wild fruits (fruit-tea 3). The preparation of the infusion tried to mimic the common preparation of tea infusions in the Canary Islands, which is quite simple [35]. Thus, 100 mL of bottled water was boiled in a glass vessel, and then one commercial packet bag of the fruit-tea (about 1.5 g) was placed in the vessel for 10 min, until it almost reached room-temperature. Afterwards, the infusion was filtered through 0.2 μm and kept in the dark at 4 ºC for no more than 48 h before being analyzed. In some experiments, the filtered infusion sample was spiked with PAHs.

2.2. Synthesis of Fe_3O_4 MNPs

α–Fe_3O_4 (magnetite) MNPs were synthesized through a modification of the alkaline co–precipitation of Fe(II) and Fe(III) method initially developed by Kang *et al.* [37]. Briefly, 2.0 g of $FeCl_2 \cdot 4H_2O$ and 5.2 g of $FeCl_3 \cdot 6H_2O$ were dissolved in 25 mL of ultrapure water containing 0.85 mL of concentrated HCl, with a nitrogen atmosphere. Then, 250 mL of 1.5 $mol \cdot L^{-1}$ NaOH was added dropwise under vigorous stirring in nitrogen atmosphere. Once the reaction was complete, the black precipitate of MNPs was separated from the reaction medium using a strong magnet. MNPs are then washed with 200 mL of ultrapure water (previously degassed) five times. The final product is re–suspended in 200 mL of ultrapure water, obtaining an estimated Fe_3O_4 MNPs concentration of ~10 $mg \cdot mL^{-1}$.

2.3. Synthesis of HKUST-1

169

170 HKUST-1 was prepared according the procedure of Wang *et al*. in 2002 [38] by
171 mixing 0.630 g of trimesic acid in 15 mL of ethanol and 1.255 g of $Cu(NO_3)_2 \cdot 2.5H_2O$ in
172 15 mL of deionized water, with stirring during 15–20 min. Afterwards, the mixture was
173 placed in a 45 mL Teflon-lined stainless steel reactor and heated at 110 ºC for 24 h. The
174 yield of the resulting HKUST-1 was of 72%, 0.716g. The purity of the crystalline
175 HKUST-1 phase was assessed by X-ray powder diffraction analysis. The complete
176 synthesis and characterization of this MOF was described in a previous work of our
177 group [7]. HKUST-1 has an intense blue color, presenting pores of 1 nm in direction
178 [*100*] and of 1.8 nm in direction [*111*]. Before its use, HKUST-1 was activated at 150
179 °C under reduced pressure during 24 h and, after that, it was always adequately
180 protected from ambient moisture to avoid its deactivation and degradation.
181

182 *2.4. Instrumentation*
183

184 The UHPLC system used was a 1260 Infinity model from Agilent Technologies
185 (Santa Clara, EEUU). The separation of PAHs was carried out with a Zorbax Eclipse
186 PAHs column (1.8 μm, 50×4.6 mm) also from Agilent Technologies. The instrument
187 was equipped with a Rheodyne 7725i valve able to supporting high pressures, with an
188 injection loop of 5 μL; quaternary pumps able to resist up to 600 Bar; a multichannel
189 fluorescence detector (FD) (able to simultaneously work with one λ_{ex} and four λ_{em}, or
190 with four λ_{ex} and one λ_{em}) equipped with a thermostat. The column thermostat was kept
191 at 30 ºC. The optimum wavelength program for the fluorescence detector is shown in
192 Table S1 of the Electronic Supplementary Material (ESM).

193 A linear gradient elution procedure was employed using a mobile phase
194 composed of ACN:water at a constant flow rate of 1 $mL \cdot min^{-1}$, starting from 80 to
195 100% of ACN (v/v) in 4 min, being then kept isocratic for another 5 min.
196 The UHPLC was controlled with the C.01.04 version of the OpenLab CDS
197 ChemStation software (Agilent), whereas data treatment was carried out with the 6.41
198 version LC Workstation software (Varian, Palo Alto, California, USA).
199 A vortex from Reax-Control Heidolph GMBH (Schwabach, Germany), and an
200 ultrasounds bath KM (Shenzhen Codyson Electrical Co., Ltd. Shenzhen, China) were
201 utilized in the microextraction procedure. The final solvent-exchange step of the
202 procedure was carried out using an air-current assisted by vacuum, with the Visiprep™
203 system of Supelco (Bellefonte, PA, USA).
204 Phase identification of the synthetized HKUST-1, α-Fe_3O_4, and
205 Fe_3O_4@HKUST-1, was carried out by X-ray powder diffraction on a X'Pert
206 Diffractometer (Panalytical, Netherlands) operating with Bragg–Brentano geometry.
207 Data collection was carried out using Cu Kα radiation (λ = 1.5418 Å) over the angular
208 range from 5.01° to 80.00° with a total exposure time of 30 min.
209 The microscopic morphology of the materials (HKUST-1, α-Fe_3O_4, and
210 Fe_3O_4@HKUST-1) was examined by a JSM6300 scanning electron microscope (JEOL,
211 Tokyo, Japan); depositing the materials on a flat surface and carbon.
212
213 *2.5. Magnetic-based dispersive micro-solid-phase extraction procedure (M-d-μSPE)*
214 Main variables of the M-d-μSPE procedure were selected through a factor by
215 factor optimization, and performing all experiments by triplicate. Under optimum
216 conditions, 20 mg of HKUST-1 and 0.5 mL of Fe_3O_4 MNPs suspension (~5 mg) are
217 placed in a Pyrex® centrifuge tube of 25 mL and subjected to 30 second of vortex to

ensure the formation of Fe_3O_4@HKUST-1 composite. Then, 20 mL of ultrapure water, water sample or fruit-tea infusion sample are added, either spiked or not with PAHs. The mixture is then subjected to ultrasounds for 5 min; followed by the placement of a prism magnet at the bottom of the flask during an equilibrium time of ~5 min, and then the supernatant is easily poured. Afterwards, the magnet is removed, and 0.5 mL of ACN are added to the tube containing MNPs together with the PAHs extracted. The tube is subjected to 5 min of vortex to perform elution of the analytes from the sorbent. The magnet is also used afterwards to facilitate the separation of the supernatant (ACN containing eluted PAHs). This step is repeated by triplicate. The total elution volume of 1.5 mL of ACN (containing PAHs) is filtered through 0.2 μm PVDF filters, subjected to dryness using a current of air assisted by a vacuum, and finally reconstituted with 0.5 mL of ACN while applying ultrasounds for 1 min. This solution is then ready for UHPLC injection.

3. Results and discussion

3.1. Chromatographic UHPLC-FD method

The analytical determination of the group PAHs selected in this work was carried out by UHPLC-FD. The optimum gradient was described in section 2.4: ACN:water at a constant flow rate of 1 $mL \cdot min^{-1}$, from 80 to 100% of ACN (v/v) in 4 min, and being then kept isocratic for another 5 min, working at 30 ºC. The optimum wavelength program utilized for the fluorescence detector is shown in Table S1 of the ESM. Figure S1 of the ESM also shows a representative chromatogram obtained under

243 optimum conditions, for a standard containing all PAHs at 3 μg L^{-1} as concentration
244 level (in ACN).

245 Table S2 of the ESM shows several quality analytical parameters of the
246 calibrations obtained by UHPLC-FD. The limits of detection (LODs) and the limits of
247 quantitation (LOQs) were calculated as the signal to noise (S/N) ratio of 3 and 10,
248 respectively; and verified by preparation of standards at such levels of concentration.
249 LODs ranged from 0.02 $\mu g \cdot L^{-1}$ for Chy to 0.08 $\mu g \cdot L^{-1}$ for I(1,2,3-cd)Py, whereas LOQs
250 varied from 0.07 $\mu g \cdot L^{-1}$ for Chy and BghiPer to 0.27 $\mu g \cdot L^{-1}$ for I(1,2,3-cd)Py. The
251 precision of the chromatographic method was evaluated injecting two standards
252 prepared at concentration levels not utilized in the calibration curve, specifically: 0.6
253 and 2.3 $\mu g \cdot L^{-1}$, but included within the calibration range. In all cases, intra-day relative
254 standard deviation (RSD, in %) values referred to the calculated concentration were
255 lower than 6.3% (n = 6). With regards to the precision of the retention times, inter-day
256 RSD values were lower than 0.88% (n = 30, 6 different days).

257

258 *3.2. Characterization of the materials*

259

260 The overall characterization of HKUST-1 was described in a previous work of
261 our group [7]. This crystalline material is obtained in the form of octahedral crystals
262 with a size between 15–50 μm, a surface area of 1068 $m^2 \cdot g^{-1}$ and a pore volume of 0.48
263 $cm^3 \cdot g^{-1}$, being these values quite similar to those previously reported by
264 Tranchemontagne *et al.* [39].

265 α-Fe_3O_4 MNPs are routinely employed in our group [10] and thus they are well
266 characterized, with majority of the particles presenting super-paramagnetism and a
267 quasi-spherical shape with diameters between 1 and 20 nm (14.9 ± 2.9 nm in average).

In the current work, we combine the MOF with α-Fe_3O_4 MNPs in a M-d-μSPE approach. Figure 1 shows the XRD diffraction pattern obtained for the Fe_3O_4@HKUST-1 phase formed when drying the solute obtained after the magnetic separation (with an external magnetic field) of a mixture of 20 mg of HKUST-1 and 0.5 mL of MNPs in 10 mL of water. Both materials, the α-Fe_3O_4 MNPs and HKUST-1 are present in the Fe_3O_4@HKUST-1 phase though they have been simply mixed and not subjected to any reaction to ensure chemical binding. Indeed, the HKUST-1 moves together with the α-Fe_3O_4 MNPs when an external magnetic field is applied. This can be clearly observed in the series of pictures included in Figure 2, and also in the video included in the ESM. Figure S2 of the ESM shows the SEM pictures obtained for bare Fe_3O_4 MNPs, bare HKUST-1, and the phase Fe_3O_4@HKUST-1 obtained as abovementioned. It seems that the MNPs agglomerated on the surface of the HKUST-1 microcrystals, acting as effective carriers when an external magnetic field is applied.

3.3. Optimization of the M-d-μSPE method

A simple factor by factor optimization was selected in this work given the *a priori* low number of factors needed in the optimization together with the simplicity of the magnetic-based extraction approaches. Thus, main parameters studied were the amount of magnetic extractant sorbent required (Fe_3O_4@HKUST-1), and the elution solvent nature, together with a further study of other variables such as the influence of the using of ultrasounds or vortex in both the extraction and the elution steps, the necessity or not of a drying step of the magnetic extractant sorbent before elution, and the number of elution steps required.

Several parameters were also fixed in the initial studies, such as the sample volume, kept at 20 mL to ensure a high preconcentration factor while allowing simple

293 manipulation; the agitation (5 min under ultrasounds) of the Fe_3O_4@HKUST-1 to
294 ensure adequate mixing with the aqueous sample, and the agitation (also 5 min under
295 ultrasounds) during the final elution step.
296
297 *3.3.1. Selection of elution solvent*
298 It has been observed that once analytes are trapped by a sorbent in d-μSPE
299 (magnetic or not), the elution step is critical to ensure quantitative desorption,
300 particularly when MOFs are used as sorbents [7]. Thus, it was first studied the influence
301 of the solvent nature in the elution procedure. These initial experiments were performed
302 fixing the amount of magnetic extractant sorbent, using 50 mg of HKUST-1 and 1 mL
303 of MNPs suspension, together with a low spiked amount of PAHs (1 $\mu g \cdot L^{-1}$) to select
304 the best elution solvent under less favorable conditions. Under these conditions, the
305 equilibration time using a magnet to ensure proper separation takes ~5 min. The
306 supernatant was discarded and the remaining material containing PAHs was subjected
307 to elution using 0.5 mL of different organic solvents: ACN, TCM, ACN:TCM (1:1,
308 v/v), DCM, ACN:DCM (1:1, v/v), and hexane. The eluting phase was evaporated to
309 dryness under air current and reconstituted with 0.5 mL of ACN only when the solvents
310 tested were not compatible with the LC mobile phase. All final eluates were filtered
311 with 0.2 μm PVDF filters followed by injection in the UHPLC-FD. Peak area of eluted
312 PAHs was used to monitor the efficiency of the method. Figure 3 shows the results
313 obtained with the solvents tested. It could be observed that, in general, ACN gave better
314 results followed by the mixture ACN:DCM (1:1, v/v). ACN was finally selected, also
315 considering that no further steps of solvent-exchange were needed for this solvent.
316
317 *3.3.2. Selection of the amount of HKUST-1 and MNPs for the M-d-μSPE method*

318 Once the nature of the elution solvent was selected, studies were performed to
319 evaluate the optimum amount of HKUST-1 and Fe_3O_4 MNPs required in the M-d-μSPE
320 method. The method was performed as abovementioned, using 20 mL of water spiked
321 with PAHs together with a certain amount of HKUST-1 and MNPs, followed by
322 ultrasounds, separation assisted with the magnet, and elution using 0.5 mL of ACN.
323 The amounts of HKUST-1 tested were: 5, 10, 20, 30, 40, 50 and 60 mg. Higher
324 amounts were not tested to ensure a microextraction procedure. In each case, these
325 amounts were accompanied by the minimum amount of Fe_3O_4 MNPs required to
326 efficiently separate the HKUST-1 together with the Fe_3O_4 MNPs from the aqueous
327 supernatant when placing the magnet. Thus, for amounts between 5 and 30 mg of
328 HKUST-1, 0.5 mL of the Fe_3O_4 MNPs suspension were required. For higher amounts of
329 HKUST-1, 1 mL of the Fe_3O_4 MNPs suspension was utilized. Figure S3 of the ESM
330 shows the results obtained. It can be observed that 20 mg of HKUST-1 (accompanied
331 by 0.5 mL of the Fe_3O_4 MNPs suspension) was enough to ensure an adequate
332 efficiency, and thus selected as optimum value.
333 To ensure that HKUST-1 was responsible of the extraction efficiency in the M-
334 d-μSPE-UHPLC-FD method and not the bare MNPs themselves, ultrapure water spiked
335 with 1 $\mu g \cdot L^{-1}$ of PAHs was subjected to the overall procedure above mentioned but
336 without the MOF: only 0.5 mL of Fe_3O_4 MNPs suspension was utilized as extractant
337 material. It was observed that the amount of PAHs eluted was almost negligible, thus
338 justifying the necessity of the MOF in this magnetic-based extraction approach.
339 The interaction of HKUST-1 and Fe_3O_4 MNPs was ensured by application of
340 vortex during 30 s in these initial experiments. Longer times were also tried at this point
341 (1, 1.5 and 5 min) to evaluate if this was exerting an influence on the extraction

342 efficiency of the method. It was observed there were no significant different in the peak
343 areas of eluted PAHs, and therefore 30 s were used in the rest of the study.
344
345 *3.3.3. Improvements in the extraction and elution steps of the M-d-μSPE method*
346 Several experiments were also conducted to improve both extraction and elution
347 steps. Thus, the method was performed applying vortex or ultrasounds during the
348 extraction step, subjecting the final Fe_3O_4@HKUST-1 to different approaches (drying
349 or not) before elution, and finally applying vortex or ultrasounds during the elution step.
350 In general, it was observed that the drying step before elution was not favorable,
351 because the Fe_3O_4@HKUST-1 got adhered to the tube walls, making difficult the
352 further interaction with the elution solvent. Figure 4 shows a summary of the results
353 obtained. It was selected the utilization of ultrasounds during the extraction step and
354 vortex for the elution step, while avoiding the drying step before elution.
355 Finally, it was studied the number of elution steps required to ensure the
356 maximum efficiency of elution. Several elution steps and modes were tried, avoiding
357 final volumes higher than 1.5 mL (to reduce long evaporation times to reach dryness
358 /reconstitution). Thus, 4 elution steps using 0.25 mL of ACN each (4 × 0.25 mL), 3
359 elution steps using 0.5 mL of ACN each (3 × 0.5 mL), and 2 elution steps using 0.75
360 mL of ACN each (2 × 0.75 mL) were tried. Results can be observed in Figure S4 of the
361 ESM. Given the obtained results, 3 elution steps (3 × 0.5 mL) were selected.
362
363 *3.4. Quality analytical parameters of the M-d-μSPE-UHPLC-FD method*
364
365 The optimum conditions of the M-d-μSPE-UHPLC-FD method for the
366 determination of PAHs are summarized in Figure 2. Thus, calibrations were obtained

using aqueous standards of PAHs (in ultrapure water) subjected to the overall M-d-μSPE-UHPLC-FD method. Figure 5(A) (top four chromatograms, each corresponding to the channel used) shows a representative chromatogram of an aqueous standard of PAHs obtained after the whole procedure. Table 1 includes several quality analytical parameters of the method. LODs and LOQs were calculated as the initial concentration in water able to generate a signal to noise ratio of three and ten, respectively, once the whole method is performed. LODs ranged from 0.8 $ng \cdot L^{-1}$ for Chy to 12 $ng \cdot L^{-1}$ for I(1,2,3-cd)Py whereas LOQs ranged from 2.7 $ng \cdot L^{-1}$ for Chy to 40 $ng \cdot L^{-1}$ for I(1,2,3-cd)Py. It should be highlighted the sensitivity obtained in this work. In another microextraction approach described in literature using Fe_3O_4@SiO_2@MIL-101 for PAHs [40] a LOQ of 9.8 $ng \cdot L^{-1}$ was described for benzo(a)anthracene (a PAH quite similar to Chy), and the remaining LOQ values for lighter PAHs ranged from 6.3 to 87.7 $ng \cdot L^{-1}$. Other literature works using MNPs and devoted to PAHs, do not normally include I(1,2,3-cd)Py in their studies. In any case, comparable and even better sensitivity is obtained with the present work, with lower sample volume requirements (20 mL), and taking into account the simplicity in the obtaining of the material. A comparative performance of the present method with other magnetic-based approaches for PAHs by HPLC has been included as supplementary material (Table S3).

The intra-day precision (as RSD in %), of the overall M-d-μSPE-UHPLC-FD procedure was assessed at two spiked levels: 45 and 450 $ng \cdot L^{-1}$ (n = 6). RSD values ranged from 2.6% for BaPy to 11% for BghiPer at the lower spiked level, and from 1.2% for Chy to 9.1% for BaPy at the higher spiked level.

The inter-day precision (as RSD in %), the relative recovery (RR, in %), and the extraction efficiency (E_R, in %) were evaluated with aqueous standards of PAHs (ultrapure water) at two different spiked levels: 10 and 45 $ng \cdot L^{-1}$ (n = 4 each day, during

3 non-consecutive days). The obtained values are included in Table 2. Average RR values of 98% and 97% were obtained at 10 and 45 $ng \cdot L^{-1}$, respectively. Regarding the extraction efficiency, E_R in %, the average values were 59% at 10 $ng \cdot L^{-1}$ and 57% at 45 $ng \cdot L^{-1}$. These values are acceptable, particularly considering that E_R values close to 100% are difficult to obtain when dealing with microextraction approaches [41]. Inter-day RSD values ranged from 3.5% to 6.3% at 10 $ng \cdot L^{-1}$ and from 4.6% to 12% at 45 $ng \cdot L^{-1}$.

3.5. Analysis of real samples

3.5.1. Water samples

Different environmental water samples, including three wastewaters and one tap water sample, were analyzed using the optimum M-d-μSPE-UHPLC-FD method. Three PAHs, namely Chy, BaPy, and DahA, could be detected but not quantified in wastewater-1. The studied PAHs were not detected neither in tap water nor the remaining wastewater samples.

Wastewater-2 was randomly selected to obtain matrix-matched calibrations using the optimized M-d-μSPE-UHPLC-FD method. Thus, Table 3 shows several quality analytical parameters obtained for the calibrations with this wastewater sample. LODs, calculated as abovementioned for ultrapure water, ranged from 1.7 $ng \cdot L^{-1}$ for BbF to 15 $ng \cdot L^{-1}$ for I(1,2,3-cd)Py. LOQs ranged from 5.6 $ng \cdot L^{-1}$ for BbF to 18 $ng \cdot L^{-1}$ for BaPy. The intra-day precision (as RSD in %), of the overall matrix-matched calibrations for wastewater-2 using M-d-μSPE-UHPLC-FD was also assessed at two spiked levels: 45 and 450 $ng \cdot L^{-1}$ (n = 6). RSD values ranged from 2.8% for BaPy to

8.9% for Chy at the lower spiked level, and from 2.1% for BaPy to 7.1% for I(1,2,3-cd)Py at the higher spiked level.

The performance of the overall method was also evaluated for tap water and the three wastewaters at different spiked levels (45 and 450 $ng \cdot L^{-1}$ for wastewater-2, 45 $ng \cdot L^{-1}$ for wastewater-1, 100 $ng \cdot L^{-1}$ wastewater-3, and 45 and 300 $ng \cdot L^{-1}$ for tap water) by means of the relative recovery, the extraction efficiency, and the inter-day precision, as it can be observed in Table 2. Average RR values (for all studied PAHs) ranged from 82% to 98% when using the calibration in ultrapure water (Table 1). If RR is evaluated for wastewater-2 using its own calibration (Table 3), the value increases from 87% to 94% (45 $ng \cdot L^{-1}$) and from 85% to 93% (450 $ng \cdot L^{-1}$), pointing out for the importance of this kind of calibration when analyzing complex samples. Regarding the E_R values with these complex samples, they range from 39% to 55% (compared to 57% and 59% in ultrapure water), which points out for a possible matrix effect. Inter-day precision presented RSD values always lower than 14%, which should be highlighted. Figure 5 includes the obtained chromatograms for spiked wastewater-2 (Figure 5(B)) and tap water (Figure 5(D)) subjected to the whole method, among other chromatograms.

3.5.2. Fruit tea infusions samples

Three different fruit tea infusions were also analyzed by M-d-μSPE-UHPLC-FD, as described in section 2.1. Only two PAHs, namely BkF and DahA, were detected but not quantified in fruit tea-3.

The infusion of fruit tea-2 was randomly selected to obtain matrix-matched calibrations using the optimized M-d-μSPE-UHPLC-FD method. Thus, Table S4 of the ESM shows several quality analytical parameters obtained for the calibrations with this fruit tea infusion sample. LODs ranged in this case from 6.1 $ng \cdot L^{-1}$ for BghiPer to 21

441 ng·L^{-1} for I(1,2,3-cd)Py, whereas LOQs ranged from 20 ng·L^{-1} for BghiPer to 70 ng·L^{-1}
442 for I(1,2,3-cd)Py. The intra-day precision (as RSD in %), of the overall matrix-matched
443 calibrations for fruit tea-2 infusion using M-d-μSPE-UHPLC-FD was also assessed at
444 two spiked levels: 45 and 450 ng·L^{-1} (n = 4). RSD values were lower than 18% and
445 19%, at 45 and 450 ng·L^{-1}, respectively.

446 The performance of the overall method was also evaluated for the three fruit
447 infusions at different spiked levels (100 ng·L^{-1} for fruit tea-1 infusion, 45 and 450 ng·L^{-1}
448 for fruit tea-2 infusion, and 450 ng·L^{-1} for fruit tea-3 infusion); by means of the
449 relative recovery, the extraction efficiency, and the inter-day precision, as it can be
450 observed in Table 2. Average RR values (for all studied PAHs) ranged from 22% to
451 45% when using the calibration in ultrapure water (Table 1), and improving up to 70%
452 (450 ng·L^{-1}) and 75% (45 ng·L^{-1}) for fruit tea-2 infusion when employing its own
453 calibration (Table S4 of ESM). This once again points out the relevance of matrix-
454 matched calibration with these complex samples. Regarding the E_R values, they are
455 much lower than those obtained with waters, ranging from 9.7%to 15%, but still
456 reaching acceptable sensitivity despite the low extraction efficiency. With regards to
457 inter-day precision, RSD values ranged from 1.6% to 22%, thus supporting the
458 precision of the method with these samples.

459 Figure 5(C) includes the obtained chromatograms for spiked fruit tea-2 infusion
460 subjected to the whole method, among other chromatograms.

461

462 **Conclusions**

463

464 A hybrid magnetic material composed of the MOF HKUST-1 and Fe_3O_4 MNPs
465 has been prepared by simple mixing and successfully utilized for first time in a M-d-

466 μSPE method together with UHPLC-FD for the analytical determination of a group of
467 heavy PAHs, including I(1,2,3-cd)Py, in a group of waters (tap water and wastewater)
468 and fruit tea infusion samples.

469 The overall method is characterized for performing adequate quantitation of
470 heavy PAHs, in terms of high sensitivity (LODs down to 0.8 $ng \cdot L^{-1}$), adequate
471 reproducibility and efficiency, while requiring low sample volumes (20 mL), low
472 amounts of sorbents (20 mg for HKUST-1 and 5 mg of Fe_3O_4 MNPs), low organic
473 solvent consumption (in both the extraction method and the chromatographic analysis),
474 while being simple: the preparation of the hybrid material and the M-d-μSPE method.

475

476 **Acknowledgements**

477 V.P. and C.R.-P. thank the MINECO for the Projects Ref. MAT2013-43101-R and
478 MAT2014-57465-R. J.H.A. and V.P. also thank funding from Fundación CajaCanarias
479 project ref. SPDs-AGUA05. C.R.-P. also thanks funding from ULL-International
480 Excellence Campus (CEI). P.R.-B. thanks her FPI PhD research contract associated to
481 the Project Ref. MAT2014-57465-R.

482

References

[1] E. Guihen, Nanoparticles in modern separation science, Trends Anal. Chem., 46 (2013) 1–14.

[2] K. Pyrzynska, Use of nanomaterials in sample preparation, Trends Anal. Chem., 43 (2013) 100–108.

[3] L.L. Vatta, R.D. Sanderson, K.R. Koch, Magnetic nanoparticles: Properties and potential applications, Pure Appl. Chem., 78 (2006) 1793–1801.

[4] K. Aguilar-Arteaga, J.A. Rodriguez, J. Barrado, Magnetic solids in analytical chemistry: A review, Anal. Chim. Acta, 674 (2010) 157–165.

[5] P. Rocio-Bautista, V. Pino, Extraction methods facilitated by the use of magnetic nanoparticles, in Volume 5, Analytical Separation Science, Wiley (2015) DOI: 10.1002/9783527678129.

[6] A. Simón de Dios, M.E. Díaz-García, Multifunctional nanoparticles: Analytical prospects, Anal. Chim. Acta, 666 (2010) 1–22.

[7] P. Rocío-Bautista, C. Martínez-Benito, V. Pino, J. Pasán, J.H. Ayala, C. Ruiz-Pérez, A.M. Afonso, The metal–organic framework HKUST-1 as efficient sorbent in avortex-assisted dispersive micro solid-phase extraction of parabens from environmental waters, cosmetic creams, and human urine, Talanta, 139 (2015) 13–20.

[8] H. Bagheri, A. Afkhami, M. Saber-Tehrani, H. Khoshsafar, Preparation and characterization of magnetic nanocomposite of Schiff base/silica/magnetite as a preconcentration phase for the trace determination of heavy metal ions in water, food and biological samples using atomic absorption spectrometry, Talanta, 97 (2012) 87–95.

[9] W. Wang, R. Ma, Q. Wu, C. Wang, Z. Wang, Magnetic microsphere-confined graphene for the extraction of polycyclic aromatic hydrocarbons from environmental water samples coupled with high performance liquid chromatography–fluorescence analysis, J. Chromatogr. A, 1293 (2013) 20–27.

[10] M.J. Trujillo-Rodríguez, V. Pino, J.L. Anderson, J.H. Ayala, A.M. Afonso, Double salts of ionic-liquid-based surfactants in microextraction: application of their mixed hemimicelles as novel sorbents in magnetic-assisted micro-dispersive solid-phase extraction for the determination of phenols, Anal. Bioanal. Chem., 407 (2015) 8753–8764.

[11] X. Zhao, Y. Shi, Y. Cai, S. Mou, Cetyltrimethylammonium bromide-coated magnetic nanoparticles for the preconcentration of phenolic compounds from environmental water samples, Environ. Sci. Technol., 42 (2008) 1201–1206.

[12] L. Chen, B. Li, Magnetic molecularly imprinted polymer extraction of chloramphenicol from honey, Food Chem., 141 (2013) 23–28.

[13] M.J. Lerma-García, M. Zougagh, A. Ríos, Magnetic molecular imprint-based extraction of sulfonylurea herbicides and their determination by capillary liquid chromatography, Microchim. Acta, 180 (2013) 363–370.

[14] B. Chen, S. Wang, Q. Zhang, Y. Huang, Highly stable magnetic multiwalled carbon nanotube composites for solid phase extraction of linear alkylbenzene sulfonates in environmental water samples prior to high-performance liquid chromatography analysis, Analyst, 137 (2012) 1232–1240.

[15] X. Cao, L. Shen, X. Ye, F. Zhang, J. Chen, W. Mo, Ultrasound-assisted magnetic solid-phase extraction based ionic liquid-coated Fe_3O_4@graphene for the determination of nitrobenzene compounds in environmental water samples, Analyst, 139 (2014) 1938–1944.

[16] J. Lei, R. Qian, P. Ling, L. Cui, H. Ju, Design and sensing applications of metal-organic framework composites, Trends Anal. Chem., 58 (2014) 71–78.

[17] Y. Cheng-Xiong, Y. Xiu-Ping, Application of metal-organic frameworks in sample pretreatment, Chin. J. Anal. Chem., 41 (2013) 1297–1301.

[18] O.M. Yaghi, M. O'Keeffe, N.W. Ockwig, H.K. Chae, M. Eddaoudi, J. Kim, Reticular synthesis and the design of new materials, Nature 423 (2003) 705–714.

[19] A. Aquino, J.A. Ferreira, S. Navickiene, K.A. Wanderley, G.F. de Sá, S.A. Júnior, Investigating the potential of metal-organic framework material as an adsorbent for matrix solid-phase dispersion extraction of pesticides during analysis of dehydrated *hyptis pectinata* medicinal plant by GC/MS, J. AOAC Inter. 95 (2012) 1338–1342.

[20] Y. Hu, C. Song, J. Liao, Z. Huang, G. Li, Water stable metal-organic framework packed microcolumn for online sorptive extraction and direct analysis of naproxen and its metabolite from urine sample, J. Chromatogr. A, 1294 (2013) 17–24.

[21] Y. Zhai, N. Li, L. Lei, X. Yang, H. Zhang, Dispersive micro-solid-phase extraction of hormones in liquid cosmetics with metal–organic framework, Anal. Methods, 6, (2014) 9435–9445.

[22] J. Xu, J. Zheng, J. Tian, F. Zhu, F. Zeng, C. Su, G. Ouyang, New materials in solid-phase microextraction, Trends Anal. Chem., 47 (2012) 68–83.

[23] Y.-Y. Wu, C.-X. Yang, X.-P. Yan, Fabrication of metal–organic framework MIL-88B films on stainless steel fibers for solid-phase microextraction of polychlorinated biphenyls, J. Chromatogr. A, 1334 (2014) 1–8.

[24] X.-Y. Cui, Z.-Y. Gu, D.-Q. Jiang, Y. Li, H.-F. Wang, X.-P. Yan, In situ hydrothermal growth of metal-organic framework 199 films on stainless steel

556 fibers for solid-phase microextraction of gaseous benzene homologues, Anal.
557 Chem., 81 (2009) 9771–9777.
558 [25] M.R. Sohrabi, Z. Matbouie, A.A. Asgharinezhad, A. Dehghani, Solid phase
559 extraction of Cd(II) and Pb(II) using a magnetic metal-organic framework, and
560 their determination by FAAS, Microchim. Acta, 180 (2013) 589–597.
561 [26] M. Taghizadeh, A.A. Asgharinezhad, M. Pooladi, M. Barzin, A. Abbaszadeh, A.
562 Tadjarodi, A novel magnetic metal organic framework nanocomposite for
563 extraction and preconcentration of heavy metal ions, and its optimization via
564 experimental design methodology, Microchim. Acta, 180 (2013) 1073–1084.
565 [27] Y. Wang, J. Xie, Y. Wu, H. Ge, X. Hu, Preparation of a functionalized magnetic
566 metal–organic framework sorbent for the extraction of lead prior to electrothermal
567 atomic absorption spectrometer analysis, J. Mater. Chem. A, 1 (2013) 8782–8789.
568 [28] Y. Wang, J. Xie, Y. Wu, X. Hu, A magnetic metal-organic framework as a new
569 sorbent for solid-phase extraction of copper (II), and its determination by
570 electrothermal AAS, Microchim. Acta, 181 (2014) 949–956.
571 [29] M. Babazadeh, R. Hosseinzadeh-Khanmiri, J. Abolhasani, E. Ghorbani-Kalhora,
572 A. Hassanpour, Solid phase extraction of heavy metal ions from agricultural
573 samples with the aid of a novel functionalized magnetic metal–organic
574 framework, RSC Adv., 5 (2015) 19884–19892.
575 [30] Y. Xu, J. Jin, X. Li, Y. Han, H. Meng, C. Song, X. Zhang, Magnetization of a
576 Cu(II)-1,3,5-benzenetricarboxylate metal-organic framework for efficient solid-
577 phase extraction of Congo Red, Microchim. Acta, 182 (2015) 2313–2320.
578 [31] G.-H. Wang, Y.-Q. Leia, H.-C. Song, Evaluation of Fe_3O_4@SiO_2–MOF-177 as an
579 advantageous adsorbent for magnetic solid-phase extraction of phenols in
580 environmental water samples, Anal. Methods, 6 (2014) 7842–7847.

581 [32] W. Zhang, Z. Yan, J. Gao, P. Tong, W. Liu, L. Zhang, Metal–organic framework
582 UiO-66 modified magnetite@silica core–shell magnetic microspheres for
583 magnetic solid-phase extraction of domoic acid from shellfish samples, J.
584 Chromatogr. A, 1400 (2015) 10–18.
585 [33] X. Chen, N. Ding, H. Zang, H. Yeung, R.-S. Zhao, C. Cheng, J. Liu, T.-W.D.
586 Chan, Fe_3O_4@MOF core–shell magnetic microspheres for magnetic solid-phase
587 extraction of polychlorinated biphenyls from environmental water samples, J.
588 Chromatogr. A, 1304 (2013) 241–245.
589 [34] S. Zhang, Z. Jiao, W. Yao, A simple solvothermal process for fabrication of a
590 metal-organic framework with an iron oxide enclosure for the determination of
591 organophosphorus pesticides in biological samples, J. Chromatogr. A, 1371
592 (2014) 74–81.
593 [35] M. Germán-Hernández, P. Crespo-Llabrés, V. Pino, J.H. Ayala, A.M. Afonso,
594 Utilization of an ionic liquid in situ preconcentration method for the determination
595 of the 15 + 1 European Union polycyclic aromatic hydrocarbons in drinking water
596 and fruit-tea infusions, J. Sep. Sci., 36 (2013) 2496–2506.
597 [36] Z. Zelinkova, T.Wenzl, The occurrence of 16 EPA PAHs in food – A review,
598 Polycycl. Aromat. Compd., 35 (2015) 248–284.
599 [37] Y.S. Kang, S. Risbud, J.F. Rabolt, P. Stroeve, Synthesis and characterization of
600 nanometer-size Fe_3O_4 and γ-Fe_2O_3 particles, Chem. Mater., 8 (1996) 2209–2211.
601 [38] Q.M. Wang, D. Shen, Martin Bülow, M.L. Lau, S. Deng, F.R. Fitch, N.O.
602 Lemcoff, J. Semanscin, Metallo-organic molecular sieve for gas separation and
603 purification, Microporous Mesoporous Mat., 55 (2002) 217–230.

[39] D.J. Tranchemontagne, J.R. Hunt, O.M. Yaghi, Room temperature synthesis of metal-organic frameworks: MOF-5, MOF-74, MOF-177, MOF-199, and IRMOF-0, Tetrahedron 64 (2008) 8553–8557.

[40] S.-H. Huo, X.-P. Yan, Facile magnetization of metal–organic framework MIL-101 for magnetic solid-phase extraction of polycyclic aromatic hydrocarbons in environmental water samples, Analyst, 137 (2012) 3445–3451.

[41] M.J. Trujillo-Rodríguez, P. Rocío-Bautista, V. Pino, A.M. Afonso, Ionic liquids in dispersive liquid-liquid microextraction, Trends Anal. Chem., 51 (2013) 87–106.

Figure Captions

Figure 1. Powder diffraction patterns of the as synthetized α-Fe_3O_4 MNPs (green line, the bottom diffraction pattern) and HKUST-1 (red line, the intermediate diffraction pattern), together with the Fe_3O_4@HKUST-1 phase formed (blue line, the top diffraction pattern).

Figure 2. Scheme of the overall M-d-µSPE procedure performed under optimized conditions. The group of sequential pictures shows the movement of the HKUST-1 together with the α-Fe_3O_4 MNPs when a magnetic field is applied, despite having simply mixed HKUST-1 and α-Fe_3O_4 MNPs.

Figure 3 Effect of the nature of the elution solvent in the final extraction efficiency of the M-d-µSPE-UHPLC-FD method, monitored as peak-area of the corresponding PAH. Experiments were performed by triplicate under the specific conditions described in the text.

Figure 4 Effect of the agitation mode used during the extraction step and during the elution step, together with the influence of the drying step before elution, monitored as peak-area of the corresponding PAHs (spiked amount: 1 $\mu g \cdot L^{-1}$ in ultrapure water). Experiments were performed by triplicate under the specific conditions described in the text.

Figure 5. Representative chromatograms obtained after the whole M-d-µSPE-UHPLC-FD procedure for: A) an aqueous standard of PAHs (0.75 $\mu g \cdot L^{-1}$ in ultrapure water), all chromatograms obtained using the four channels have been plotted; B) wastewater-2 spiked with PAHs (0.10 $\mu g \cdot L^{-1}$), only channel A has been plotted; C) tap water spiked with PAHs (0.30 $\mu g \cdot L^{-}$

637 ^{1}), only channel A has been plotted; and D) fruit tea-2 spiked with PAHs

638 (0.75 $\mu g \cdot L^{-1}$), only channel A has been plotted.

Table 1. Quality analytical parameters of the overall M-d-μSPE-UHPLC-FD method using aqueous standards of PAHs (ultrapure water).

PAHs	Working range[a] (μg·L^{-1})	R	$S_{y/x}$[b]	Slope ± SD[c]	Intercept ± SD[c]	LOD (ng·L^{-1})	LOQ (ng·L^{-1})	RSD (%) Level 1[d]	Level 2[e]
BaA	0.01 – 0.75	0.9997	0.07	8.6 ± 0.1	0.10 ± 0.04	1.8	6.0	8.7	4.6
Chy	0.01 – 0.75	0.9990	0.30	24.4 ± 0.6	0.9 ± 0.2	0.8	2.7	7.6	1.2
BbF	0.01 – 0.75	0.9978	0.14	6.1 ± 0.2	0.4 ± 0.1	1.8	6.0	4.6	1.9
BkF	0.01 – 0.75	0.9988	0.20	11.9 ± 0.3	0.4 ± 0.1	1.3	4.3	6.5	8.6
BaPy	0.01 – 0.75	0.9985	0.17	11.0 ± 0.3	0.2 ± 0.1	4.6	15	2.6	9.1
DahA	0.01 – 0.75	0.9989	0.12	9.4 ± 0.2	0.4 ± 0.1	1.3	4.3	10	7.5
BghiPer	0.01 – 0.75	0.9986	0.13	7.8 ± 0.2	0.2 ± 0.1	1.2	4.0	11	3.5
I(1,2,3-cd)Py	0.05 – 0.75	0.9991	0.01	1.03 ± 0.02	0.01 ± 0.03	12	40	9.0	1.5

[a]concentration of PAHs in ultrapure water

[b]standard deviation of the residuals (or error of the estimate)

[c]errors of slopes and intercepts for n = 7 calibration levels

[d]intra-day precision (as RSD, in %) evaluated at 45 ng·L^{-1} (n = 6), which is a concentration level not used in the calibration plot

[e]intra-day precision (as RSD, in %) evaluated at 450 ng·L^{-1} (n = 6), which is a concentration level not used in the calibration plot

640 **Table 2.** Performance of the overall M-d-µSPE-UHPLC-FD method in terms of relative

641 recovery, extraction efficiency, and inter-day precision.

	Spiked level ($ng \cdot L^{-1}$)	**Average E_R[a,b] (all PAHs, inter-day)**	**Average RR[a,c] (%) (all PAHs, inter-day)**	**Range of inter-day RSD[a,d] (%)**
Ultrapure water	10[e]	59[e]	98[e]	3.5 – 6.3
	45	57	97	4.6 – 12
Wastewater-1	45	39	98	1.2 – 9.0
Wastewater-2	45	52	87 (94[f])	6.1 – 14
	450	55	85 (93[f])	2.1 – 11
Wastewater-3	100	45	83	1.3 – 9.4
Tap water	45	43	82	5.9 – 9.0
	300	44	83	2.5 – 8.2
Fruit tea-1	100	9.7	22	1.6 – 14
Fruit tea-2	45[e]	15[e]	45[e] (75[g])	7.2 – 17
	450	8.3	38 (70[g])	6.3 – 18
Fruit tea-3	45[e]	10[e]	40[e]	13 – 22

[a]n = 4 each day, during 3 non-consecutive days

[b]E_R values were calculated using the chromatographic calibrations (UHPLC-FD) as described in the text

[c]RR values were calculated using the calibrations obtained with PAHs aqueous standards (ultrapure water)

[d]minimum and maximum RSD values

[e]I(1,2,3-cd)Py is excluded in the average at this spiking level (lower than its LOQ)

[f]RR values in parenthesis were calculated using the matrix-matched calibrations obtained with wastewater-2

[g]RR values in parenthesis were calculated using the matrix-matched calibrations obtained with fruit tea-2 infusion

642

643 **Table 3.** Matrix-matched calibrations for the whole M-d-µSPE-UHPLC-FD method using wastewater-2.

PAHs	Working range[a] (µg·L^{-1})	R	$S_{y/x}$[b]	Slope ± SD[c]	Intercept ± SD[c]	LOD (ng·L^{-1})	LOQ (ng·L^{-1})	RSD (%) Level 1[d]	Level 2[e]
BaA	0.025 – 0.60	0.9998	0.04	7.7 ± 0.1	-0.01 ± 0.03	4.1	14	4.8	4.9
Chy	0.025 – 0.60	0.9990	0.32	25.5 ± 0.6	-0.2 ± 0.2	2.0	6.7	8.9	5.0
BbF	0.025 – 0.60	0.9978	0.19	10.6 ± 0.3	0.1 ± 0.1	1.7	5.6	7.6	6.6
BkF	0.025 – 0.60	0.9975	0.34	17.3 ± 0.6	0.3 ± 0.2	2.1	7.0	8.2	5.4
BaPy	0.025 – 0.60	0.9967	0.64	29 ± 1	0.5 ± 0.4	5.4	18	2.8	2.1
DahA	0.025 – 0.60	0.9966	0.27	11.8 ± 0.5	0.3 ± 0.2	2.8	9.3	5.6	3.2
BghiPer	0.025 – 0.60	0.9986	0.15	10.2 ± 0.3	0.2 ± 0.1	2.4	8.0	8.0	6.8
I(1,2,3-cd)Py	0.060 – 0.60	0.9963	0.03	1.1 ± 0.1	0.02 ± 0.02	15	50	-	7.1

[a]concentration of PAHs in wastewater-2

[b]standard deviation of the residuals (or error of the estimate)

[c]errors of slopes and intercepts for n = 6 calibration levels

[d]intra-day precision (as RSD, in %) evaluated at 45 ng·L^{-1} (n = 4), which is a concentration level not used in the calibration plot

[e]intra-day precision (as RSD, in %) evaluated at 450 ng·L^{-1} (n = 4), which is a concentration level not used in the calibration plot

644

Figure S1. Optimum UHPLC-FD chromatogram obtained for the group of PAHs (standard of 3 µg·L^{-1} in acetonitrile)

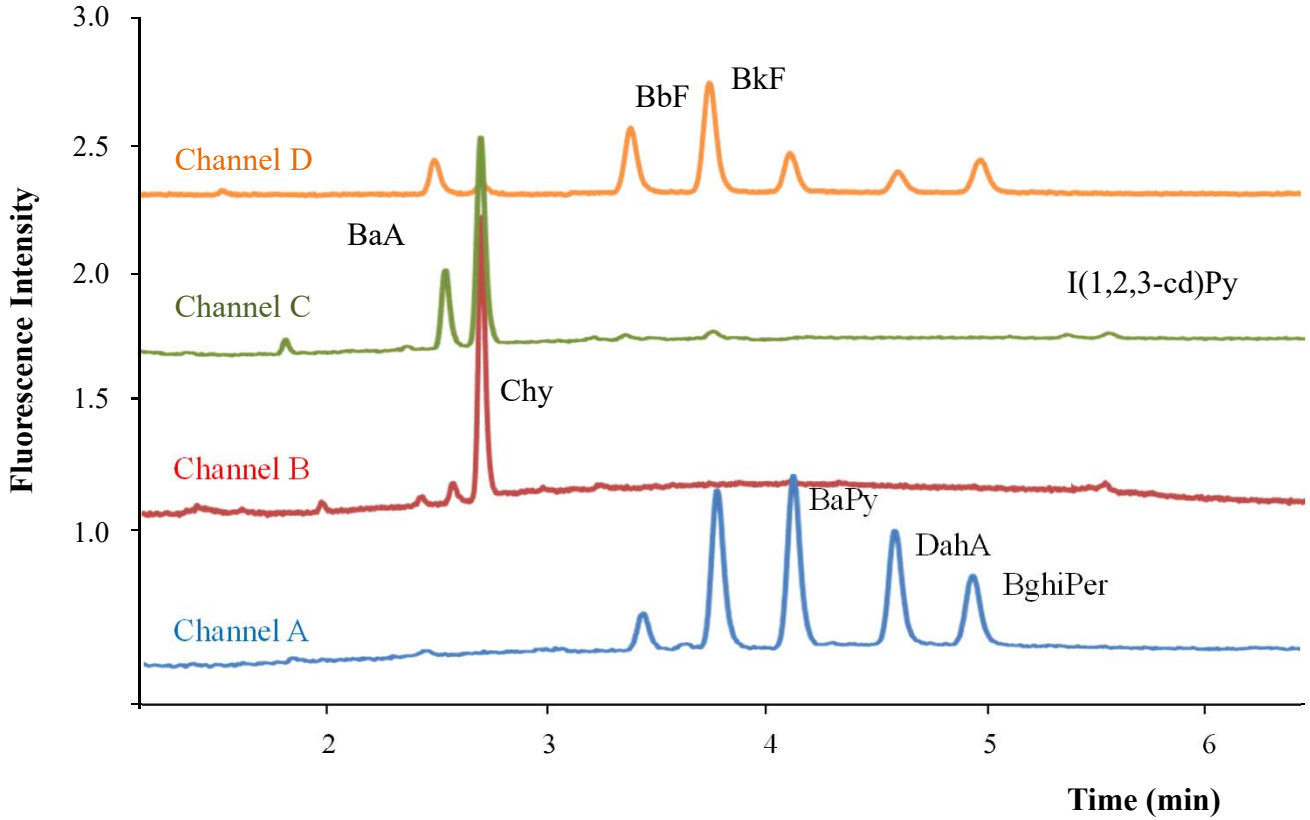

Figure S2. SEM micrographs of the as synthetized crystallites of A) HKUST-1 and B) bare Fe_3O_4 MNPs, together with the Fe_3O_4@HKUST-1 phase formed (C)).

A) HKUST-1 **B)** Bare Fe_3O_4 MNPs **C)** Fe_3O_4@HKUST-1 MNPs

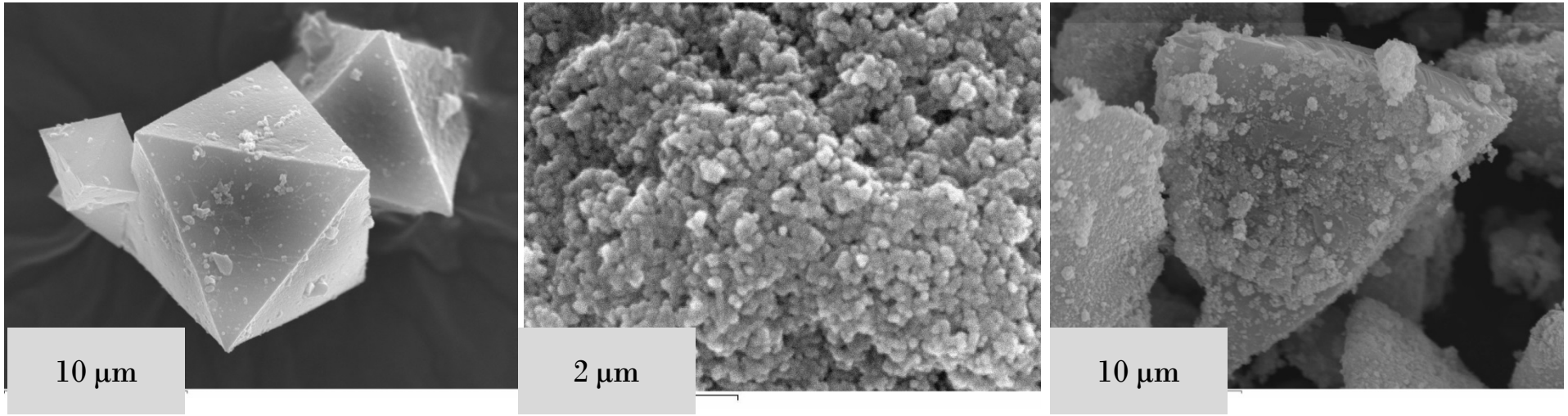

Figure S3. Effect of the amount of HKUST-1 in the performance of the method. Peak area values correspond to the eluted PAHs (using 0.5 mL of ACN for the elution step) by M-d-µSPE-UHPLC-FD (n = 3), for a initial spiked amount of PAHs of 0.8 µg·L^{-1} in ultrapure water. Remaining experimental conditions as described in the text.

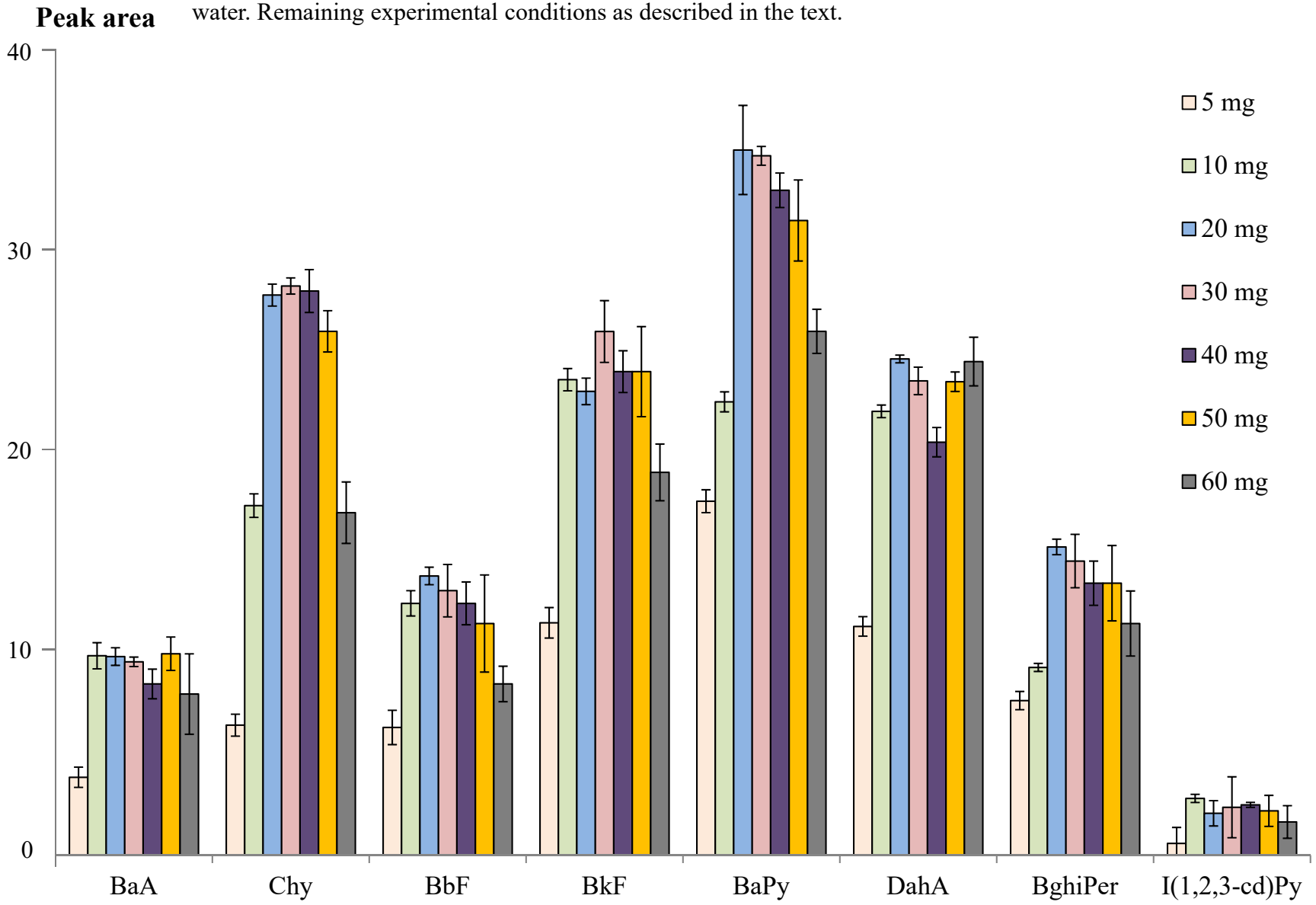

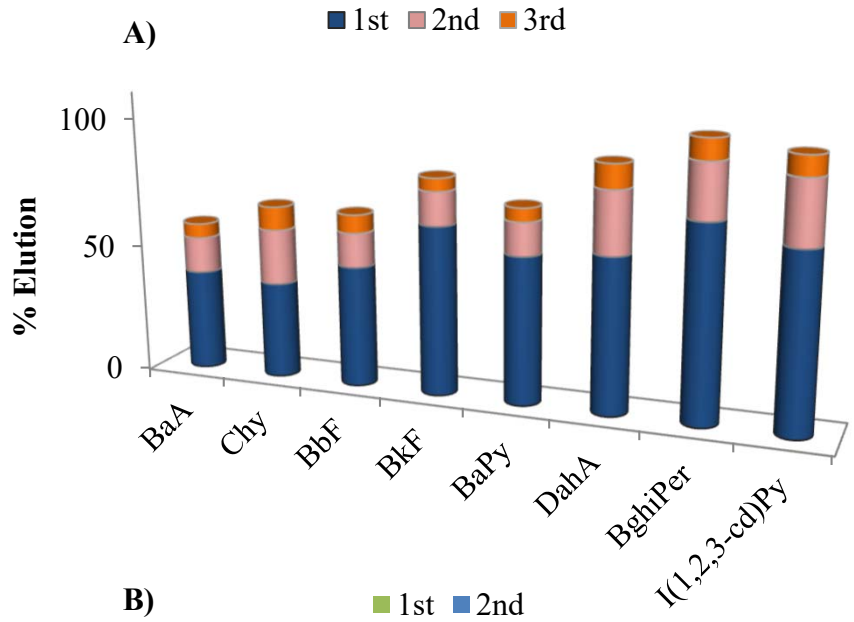

PAH	Average Elution Efficiency (%)
BaA	58.3
Chy	67.5
BbF	67.0
BkF	83.3
BaPy	74.8
DahA	93.1
BghiPer	104
I(1,2,3-cd)Py	100

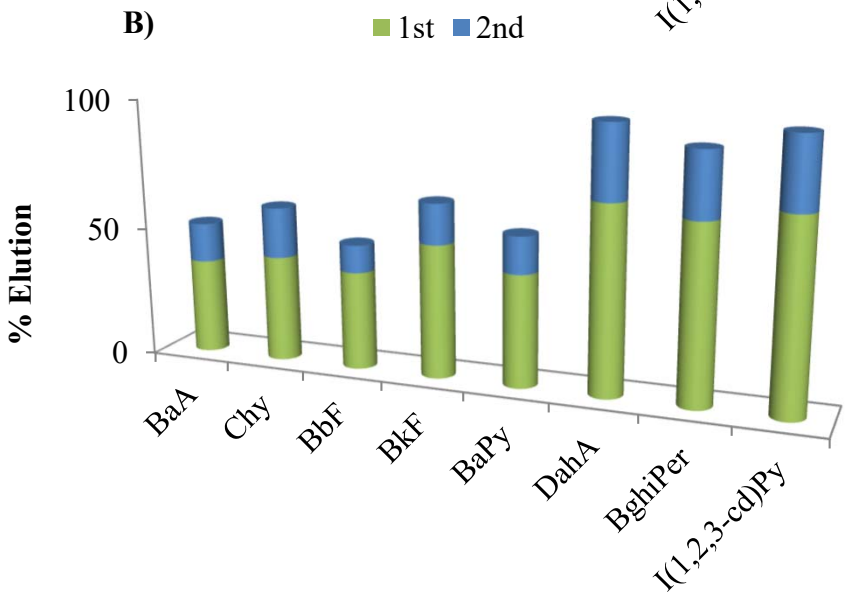

PAH	Average Elution Efficiency (%)
BaA	51.2
Chy	59.9
BbF	48.2
BkF	66.8
BaPy	57.3
DahA	105
BghiPer	92.7
I(1,2,3-cd)Py	102

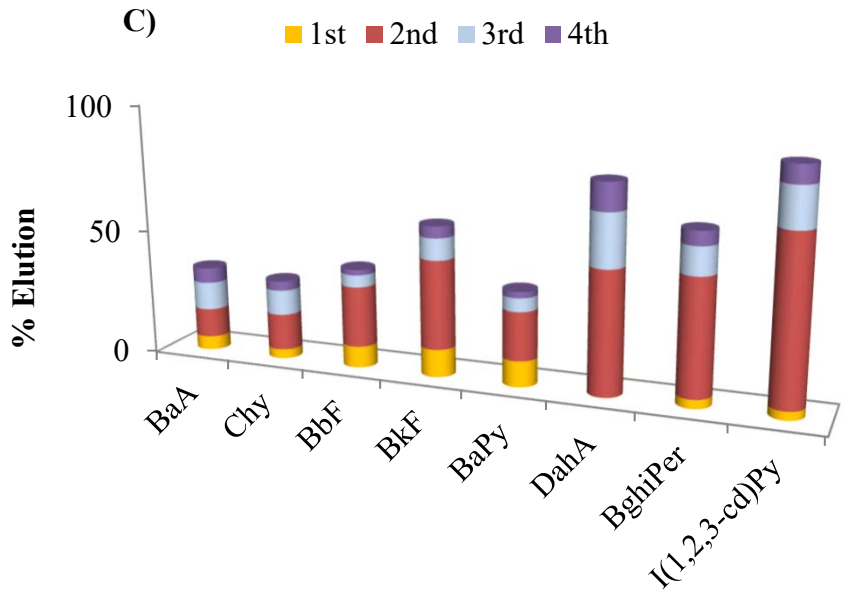

PAH	Average Elution Efficiency (%)
BaA	34.0
Chy	31.8
BbF	39.6
BkF	59.4
BaPy	37.4
DahA	80.9
BghiPer	66.0
I(1,2,3-cd)Py	91.6

Figure S4. A) Three elution steps with 0.5 mL of ACN each; B) two elution steps with 0.75 mL ACN each; and C) four elution steps with 0.25 mL of ACN each. The spiked amount of PAHs in water was 1 $\mu g \cdot L^{-1}$. Remaining conditions as described in the text.

Table S1. Wavelength program used in the multichannel fluorescence detector, presenting 4 channels (A, B, C, and D).

PAH	Tiempo (min)	λ_{ex} (nm)	λ_{em}[a] (nm)
	Initial	270	A: 330; B: 375; C: 385; D: 443
BaA			
Chy			
	2.8	275	
	3.0		A: 406; B: 375; C: 385; D: 443
	3.1		A: 406; B: 375; C: 385; D: 451
BbF			
BkF			
BaPy			
	4.3		A: 406; B: 375; C: 496; D: 451
	4.4	288	
DahA			
BghiPer			
I(1,2,3-cd)Py			

[a]changes performed in the emission channels (A, B, C or D) have been underlined.

One single modification is permitted at a time by the fluorescence detector.

Table S2. Several quality analytical parameters of the calibrations obtained by UHPLC-FD for the PAHs selected.

PAHs	Retention time ± SD[a]	Working range (µg·L^{-1})	Slope ± SD[b]	Intercept ± SD[b]	R^2	$S_{y/x}$[c]	LOD (µg·L^{-1})	LOQ (µg·L^{-1})	RSD (%) Level 1[d]	RSD (%) Level 2[e]
BaA	2.53 ± 0.02	0.1 ± 2.5	0.64 ± 0.01	0.05 ± 0.02	0.997	0.03	0.03	0.09	2.0	5.6
Chy	2.92 ± 0.02	0.1 ± 2.5	1.83 ± 0.02	-0.002 ± 0.031	0.997	0.05	0.02	0.07	1.3	3.8
BbF	3.55 ± 0.03	0.1 ± 2.5	0.69 ± 0.01	0.02 ± 0.02	0.999	0.03	0.06	0.09	3.0	3.9
BkF	3.83 ± 0.02	0.1 ± 2.5	1.21 ± 0.01	0.08 ± 0.02	0.999	0.03	0.03	0.09	1.3	2.9
BaPy	4.32 ± 0.03	0.1 ± 4.0	1.95 ± 0.05	-0.23 ± 0.11	0.998	0.15	0.03	0.08	5.8	6.3
DahA	4.81 ± 0.03	0.2 ± 3.0	0.69 ± 0.02	0.24 ± 0.03	0.997	0.04	0.04	0.14	3.1	5.2
BghiPer	5.19 ± 0.05	0.1 ± 4.0	0.63 ± 0.01	0.04 ± 0.01	0.997	0.02	0.03	0.07	3.0	4.2
I(1,2,3-cd)Py	5.47 ± 0.03	0.5 ± 8.0	0.08 ± 0.01	0.01 ± 0.01	0.998	0.01	0.08	0.27	5.3	3.6

[a]standard deviation of the retention times for n = 30

[b]errors of slopes and intercepts for n = 8 calibration levels

[c]standard deviation of the residuals (or error of the estimate)

[d]intra-day precision (as RSD, in %) evaluated at 0.6 µg·L^{-1} (n = 6), which is a concentration level not used in the calibration plot

[e]intra-day precision (as RSD, in %) evaluated at 2.3 µg·L^{-1} (n = 6), which is a concentration level not used in the calibration plot

Table S3. Comparative performance of the method proposed in this work with other M-d-µSPE methods for the determination of PAHs.

Sorbent (amount) / comments	**PAHs (nº) / comments**	**Sample (volume)**	**Determination**	**LODs ($ng \cdot L^{-1}$)**	**Reference**
Fe_3O_4@SiO_2-MIL101 (1 + 0.6 mg) / facilitated by microwaves	Lighter PAHs (6)	water (20 mL)	HPLC-DAD	2.8 – 27.2	[40]
Fe_3O_4@poly(St-DVB-*co*-4VBSS)[b] (10 mg)	Lighter PAHs (6)	water (10 mL)	UHPLC-DAD	1.92 – 13.6 $\mu g \cdot L^{-1}$	J. Chromatogr. A, 1247 (2012) 1–9
Fe_3O_4/C (50 mg)	Heavy PAHs (7) / I(1,2,3-cd)Py not studied	water (1000 mL)	HPLC-FD	0.2 – 0.6	J. Chromatogr A, 1217 (2010) 4757–4764
Fe_3O_4@poly(DA)[a] (250 mg)	Heavy PAHs (6) / I(1,2,3-cd)Py not studied	water (500 mL)	HPLC-FD	0.5 – 1.9	J. Chromatogr A, 1283 (2013) 20–26
Fe_3O_4@poly(PtBMA-*b*-PGMA)[c] (50 mg)	Heavy PAHs (3) / I(1,2,3-cd)Py not studied	water (50 mL)	HPLC-UV	2.4 – 6.3	J. Chromatogr A, 1316 (2013) 1–7
Fe_3O_4@HKUST-1 (5 + 20 mg)	Heavy PAHs (8) / including I(1,2,3-cd)Py	water & fruit tea infusion (20 mL)	UHPLC-FD	2.7 – 4.6[d]	This work

[a]poly(dopamine)

[b]poly(styrene-divinylbenzene with co-monomer: 4-vinylbenzene sulfonic acid sodium salt)

[c]poly(tert-butyl methacrylate)-block-poly(glycidyl methacrylate)

[d]range in absence of I(1,2,3-cd)Py

Table S4. Matrix-matched calibrations for the whole M-d-μSPE-UHPLC-FD method using the infusion of fruit tea-2.

PAHs	Working range[a] (μg·L^{-1})	R	$S_{y/x}$[b]	Slope ± SD[c]	Intercept ± SD[c]	LOD (ng·L^{-1})	LOQ (ng·L^{-1})	RSD (%) Level 1[d]	Level 2[e]
BaA	0.040 – 0.630	0.998	0.04	3.1 ± 0.1	0.14 ± 0.02	9.9	33	18	18
Chy	0.040 – 0.630	0.995	0.16	4.3 ± 0.3	0.51 ± 0.11	8.9	30	14	19
BbF	0.040 – 0.630	0.997	0.04	1.3 ± 0.1	0.13 ± 0.02	9.4	31	9.9	14
BkF	0.040 – 0.630	0.996	0.05	2.2 ± 0.1	0.23 ± 0.03	10	33	18	12
BaPy	0.040 – 0.630	0.970	0.24	2.2 ± 0.5	0.32 ± 0.16	8.7	29	12	10
DahA	0.040 – 0.630	0.995	0.05	0.9 ± 0.1	0.34 ± 0.04	14	39	13	14
BghiPer	0.040 – 0.630	0.989	0.12	0.6 ± 0.3	0.26 ± 0.11	6.1	20	13	12
I(1,2,3-cd)Py	0.080 – 0.630	0.998	0.01	0.14 ± 0.02	0.01 ± 0.01	21	70	-	13

[a]concentration of PAHs in the filtrated infusion fruit tea-2

[b]standard deviation of the residuals (or error of the estimate)

[c]errors of slopes and intercepts for n = 6 calibration levels

[d]intra-day precision (as RSD, in %) evaluated at 45 ng·L^{-1} (n = 4), which is a concentration level not used in the calibration plot

[e]intra-day precision (as RSD, in %) evaluated at 450 ng·L^{-1} (n = 4), which is a concentration level not used in the calibration plot